Fiducial Reference Measurements for Ground-Based DOAS Air-Quality Observations

ESA Contract No. 4000135355/21/I-DT-lr

Deliverable D1.1:

Technical note (TN) on estimation of uncertainty methodology

Date: 14/10/2022

Version: 1c

Contributing authors:

F. Hendrick, H. Yu, M. Friedrich, M. Van Roozendael (IASB-BIRA)
A. Richter and Tim Bösch (IUP-UB)
U. Friess (IUP-HD)
A. Piters (KNMI)
T. Wagner and J. Pukite (MPIC)
M. Navarro and M. Yela (INTA)
A. Bais and D. Karagkiozidis (AUTH)

Content

Acronyms and abbreviations

Acronyms and abbreviated terms that are specific for this document can be found below.

AMF	Air Mass Factor
CCD	Charge-coupled Device
CPS	Central Processing System
DISORT	Discrete-Ordinate Radiative Transfer model
DOAS	Differential Optical Absorption Spectroscopy
DOFS	Number of Degrees of Freedom for Signal
DSCD	Differential Slant Column Density
EDE	Extra-DSCD error
FRM_4DOAS	Fiducial Reference Measurements for Ground-Based DOAS Air-Quality Observations
LIDORT	LInearized Discrete Ordinate Radiative Transfer
MYSTIC	Monte Carlo code for the phYSically correct Tracing of photons In Cloudy atmospheres
OEM	Optimal Estimation Method
QA/QC	Quality Assurance/Quality Control
RMS	Root mean square
RTM	Radiative transfer model
SLIMCAT	Single Layer Isentropic Model of Chemistry And Transport
SNR	Signal-to-noise Ratio
SZA	Solar zenith angle
TN	Technical Note
VCD	Vertical Column Density
WF	Weighting Function
WP	Work Package
XS	Cross-section

1 Introduction

As part of the FRM$_4$DOAS Phase I project, it was found that stratospheric NO_2 vertical profiles retrieved from high signal to noise ratio research-grade instruments have a tendency to show unrealistic oscillations, more precisely a double peak structure. Through different retrieval sensitivity tests, this feature was found to be related to the (very) low random error on the twilight zenith-sky NO_2 DSCD derived with such instruments. Further efforts towards a better characterisation of the different error sources related to the profile retrieval were found necessary in order to obtain a consolidated stratospheric NO_2 ready for implementation in the FRM$_4$DOAS central processing chain.

The main objective of the FRM$_4$DOAS-2.0 WP1 is to develop different approaches for (1) better characterizing the uncertainty of twilight zenith-sky NO_2 DSCDs, and (2) investigating the impact of this uncertainty on the retrieved profiles and VCDs. This technical note (TN) describes these different approaches (see Sect. 2) and corresponding results (see Sect. 3). Overall assessment of these approaches and recommendations for the consolidation of the FRM$_4$DOAS stratospheric NO_2 profiling algorithm are presented in Sect. 4. References are given in Sect. 5.

2 Methodology

The methodology for consolidating the FRM$_4$DOAS stratospheric NO_2 product is based on the following approaches and related tasks:

Approach 1: Better estimation of the random uncertainty on twilight zenith-sky NO_2 DSCDs

- Sensitivity tests: increase or decrease of the DOAS fit errors and impact on the retrieved profile and control parameters (DOFS, RMS)
- Collection of the NO_2 DOAS fit errors from the different instruments
- Collection of the SZA range and sampling at twilight of the different partners' instruments/Comparison with criteria from Hendrick et al. (2004)
- Sensitivity tests with respect to the linearised dependence in temperature of the NO_2 cross-sections (XS) available data sources

Approach 2: Better estimation of the uncertainty related to the forward modelling

- Determination of the impact of the Earth' sphericity on AMF calculation
- Check the impact of the photochemical correction included in the forward model and its related uncertainty on the retrieved profiles

Approach 3: Characterization of the 'atmospheric noise' related to clouds and tropospheric NO_2

- Use of the extra-DSCD error approach (polynomial fit through consecutive zenith DSCDs) and verification using fast zenith-sky measurements at the Bremen station

The results obtained in these different tasks are described in the next section.

3 Results

3.1 Approach 1: Better estimation of the random uncertainty on twilight zenith-sky NO_2DSCDs

3.1.1 Collection of the DOAS fit errors from the different FRM$_4$DOAS instruments

The DOAS fit uncertainties on the twilight zenith-sky NO_2 DSCDs have been collected for the instruments included in the CPS and providing stratospheric NO_2 vertical profiles (see Figure 1).

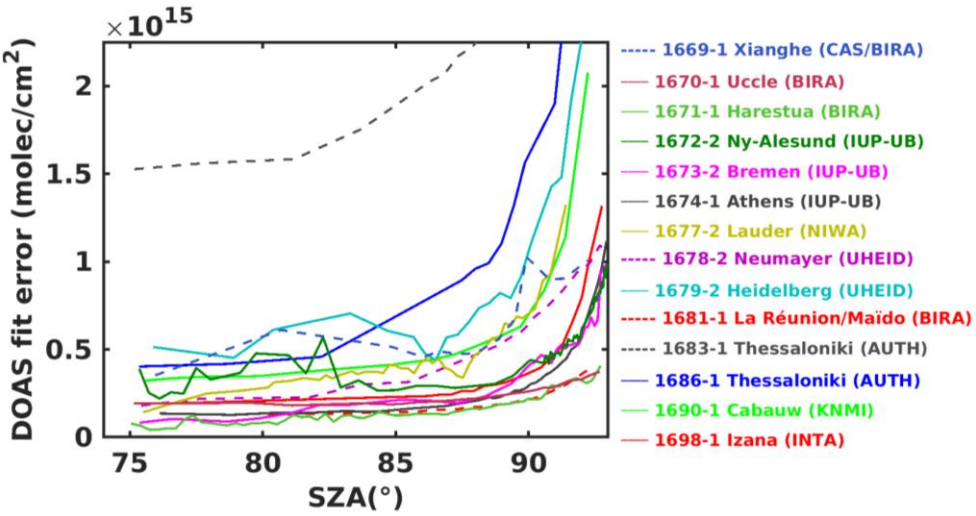

Figure 1: NO_2 DOAS fit uncertainties for the different instruments included in the CPS. Except for Lauder (08/12/2020 sunset) and Neumayer (03/02/2020 sunset), those DOAS fit uncertainties correspond to measurements taken on 20/06/2019 sunset.

As expected, the DOAS fit uncertainties from commercial and/or lower signal to noise ratio instruments (Lauder, Heidelberg, Thessaloniki, Cabauw) are larger than those from high signal to noise ratio instruments. The impact of those differences in the retrieved stratospheric NO_2 profile shapes and VCDs have been assessed through sensitivity tests where the NO_2 DOAS fit errors will be artificially increased (for high SNR instruments) or decreased (for lower SNR instruments) (Section 3.1.3).

3.1.2 Collection of the SZA range and sampling at twilight from the different FRM$_4$DOAS instruments

As shown in Hendrick et al. (2004), the SZA range and sampling at twilight are two important parameters that can influence the quality of the stratospheric NO_2 vertical profile retrieval. For instance, a SZA sampling above 89°SZA of 0.25° instead of 1° can lead to a DOFS increase of up to 30%. Having an SZA upper limit well above 90° can also significantly increase the DOFS (see left plot in Figure 2 below). Both parameters have been collected for the instruments included in the CPS providing stratospheric NO_2 vertical profiles (see right plot in Figure 2 below). As can be seen, all the instruments meet the minimum criteria for retrieving stratospheric NO_2 profiles, both in terms of SZA upper limit (93° or higher for all the instruments) and SZA sampling (less than 0.5° above 86°SZA for most of the instruments; below 85°SZA, the sampling is coarser for most of the MAX-DOAS instruments but it is not an issue for the profile

retrieval). So changes in the measurement sequence for the different instruments do not seem to be needed at this stage.

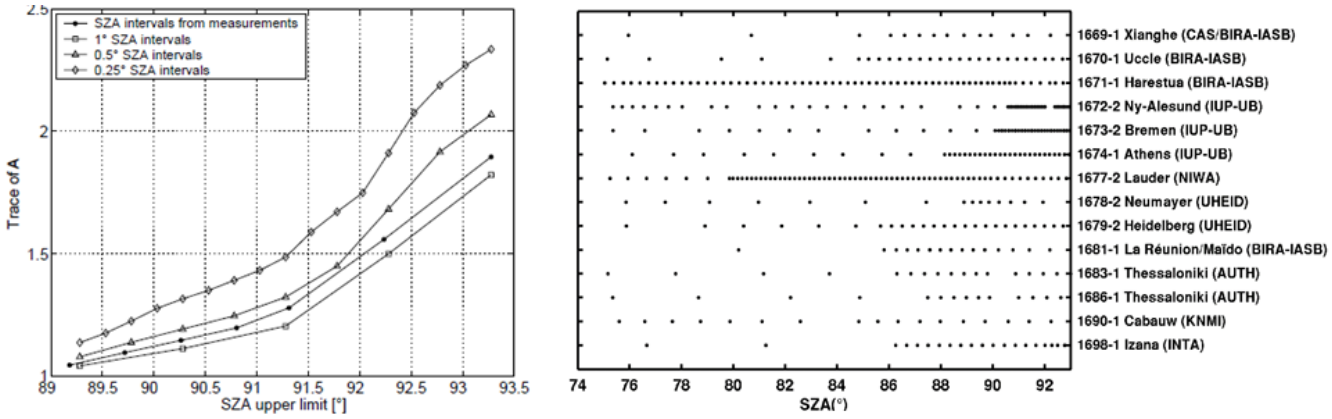

Figure 2: (Left plot) Impact of the SZA sampling (SZA upper limit and SZA intervals) of the measurements on the number of independent pieces of information (trace of the averaging kernels matrix A). Synthetic measurements with fixed SZA intervals have been generated by using a polynomial fit through the sunset Harestua 25 May 2001 measurements and interpolating on the desired SZA grid (from Hendrick et al., 2004). (Right plot) SZA range and sampling for the different instruments included in the CPS.

3.1.3 Increasing or decreasing the random uncertainty on NO_2 DSCDs

Sensitivity tests on the OEM-based stratospheric NO_2 profile retrieval were carried out by artificially increasing or decreasing the DOAS fit errors and assessing the corresponding impact on the retrieved profiles and control parameters (DOFS, RMS). Their main objective is not to do a tuning for fixing the OEM settings but for a given S_a, to estimate the random error threshold at which a double peak pattern appears. For the study cases investigated (4 August 2018 sunset measurements from the Bremen high SNR research grade and Heidelberg lower SNR Airyx instruments; variance of 20% of the a priori profile on the diagonal elements of the S_a matrix), an average random error of ~1% (or ~1.2e15 molec/cm^2) on the NO_2 DSCDs at SZA larger than 85° seems to be the threshold value at which the retrieval becomes unstable and a double peak appears in the retrieved profiles (see Figure 3). We see also that for the present study cases, double peak patterns correspond to DOFS larger than 2.

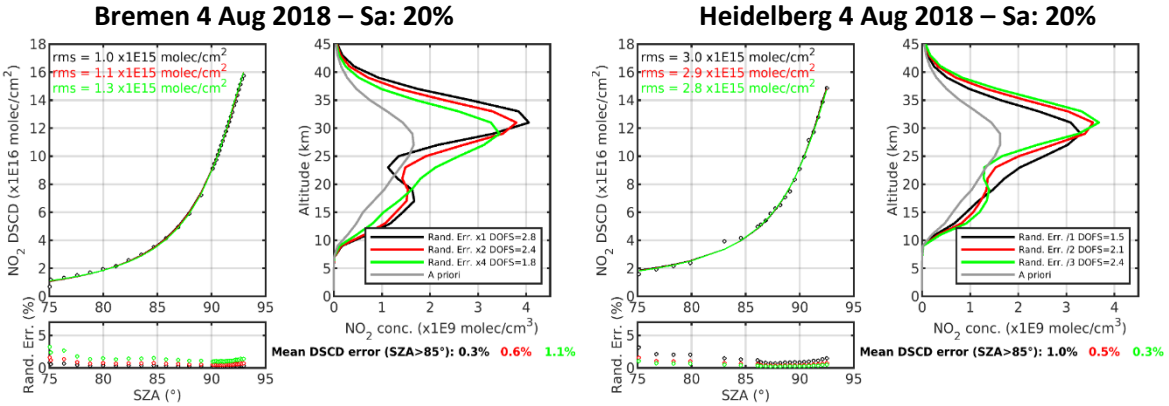

Figure 3: Results of the sensitivity tests where NO_2 DSCD uncertainties are decreased (Bremen 4 Aug 2018; left plot) or increased (Heidelberg 4 Aug 2018; right plot) with constant Sa matrix fixed to 20% of the a priori profile.

This double peak pattern could be related to issue(s) in the forward modelling, in particular a potential problem with the photochemical correction applied in the retrieval. This is investigated in Section 3.2.

3.1.4 Sensitivity tests with respect to the linearised dependence in temperature of the different NO_2 XS data sources

For this sensitivity test, the linearised dependence in temperature of the NO_2 cross sections in the visible range (460nm) is derived using three different cross section data sources (Bogumil et al., 2000; Burrows et al., 1998; Vandaele et al., 1998 which is used as baseline in the CPS). As can be seen in Figure 4, a good agreement is found between the three data sets, with a linear dependence varying from -0.29%/K for Bogumil et al. (2000) to -0.32%/K for Burrows et al. (1998) and Vandaele et al. (1998). For typical stratospheric temperature range around 220K (which is e.g. ~190-237K at 60°N at the altitude of the NO_2 concentration peak (~27km)), the uncertainty related to the NO_2 XS source on the temperature dependence is therefore small (~0.4-0.9%). Based on this test, it seems not necessary to add this additional uncertainty source to the uncertainty budget of the stratospheric NO_2 product.

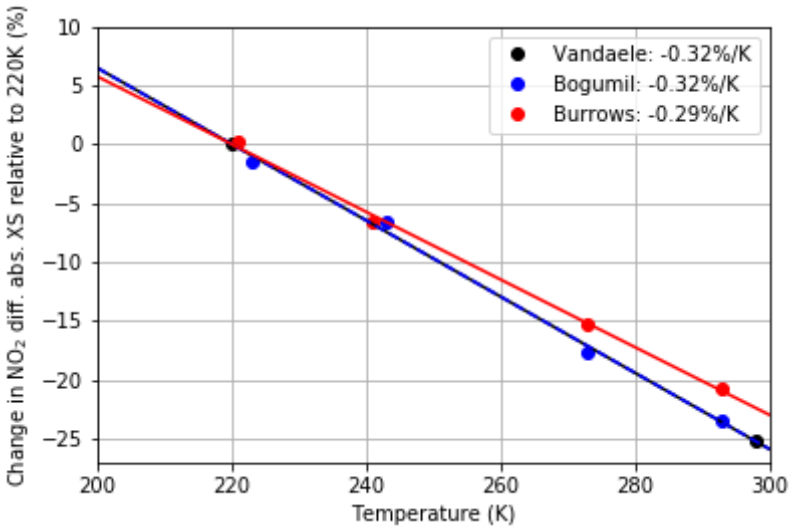

Figure 4: Change (in %) in NO_2 differential absorption XS as a function of the temperature for the three selected NO_2 XS sources. The linearised temperature dependences are normalized with respect to 220K.

3.2 Approach 2: Better estimation of the uncertainty related to the forward modelling

3.2.1 Determination of the impact of the Earth' sphericity on AMF calculation

The impact of the sphericity on twilight zenith-sky NO_2 AMFs has been assessed through comparisons of NO_2 AMFs simulated using four different RTMs:

- 2 full spherical models: McArtim v3 (https://www.tim-deutschmann.de/McArtim/) and MYSTIC (Emde et al., 2022) Monte Carlo codes in which a full spherical geometry is implemented for both direct and diffuse light.
- 2 pseudo-spherical models: DISORT (Mayer and Kylling, 2005), which is currently used as forward model in the stratospheric NO_2 profiling, and LIDORT (Spurr, 2006). In both models, spherical and plane parallel geometries are implemented for direct light and diffuse light, respectively.

The four RTMs have been initialised with the following common input files and settings:

- Ground zenith-sky viewing geometry
- Wavelengths: 326, 354, 460, 700, 1000, and 2000 nm
- SZA: 0 to 65° with 5° step, then 66 to 95° with 1° step
- Fixed NO_2, O_3, pressure, and temperature vertical profiles and altitude grid (0-90km/step 2km) taken from SLIMCAT/PSCBOX stacked 1D photochemical model
- Surface albedo: 0 and 7%
- No aerosol

By comparing the difference between NO_2 AMFs calculated with full spherical and pseudo-spherical models, the contribution of the sphericity on the diffuse light can be quantified.Typical examples of NO_2 AMF comparison results at 326, 460, and 1000 nm are shown in Figure 5 below.

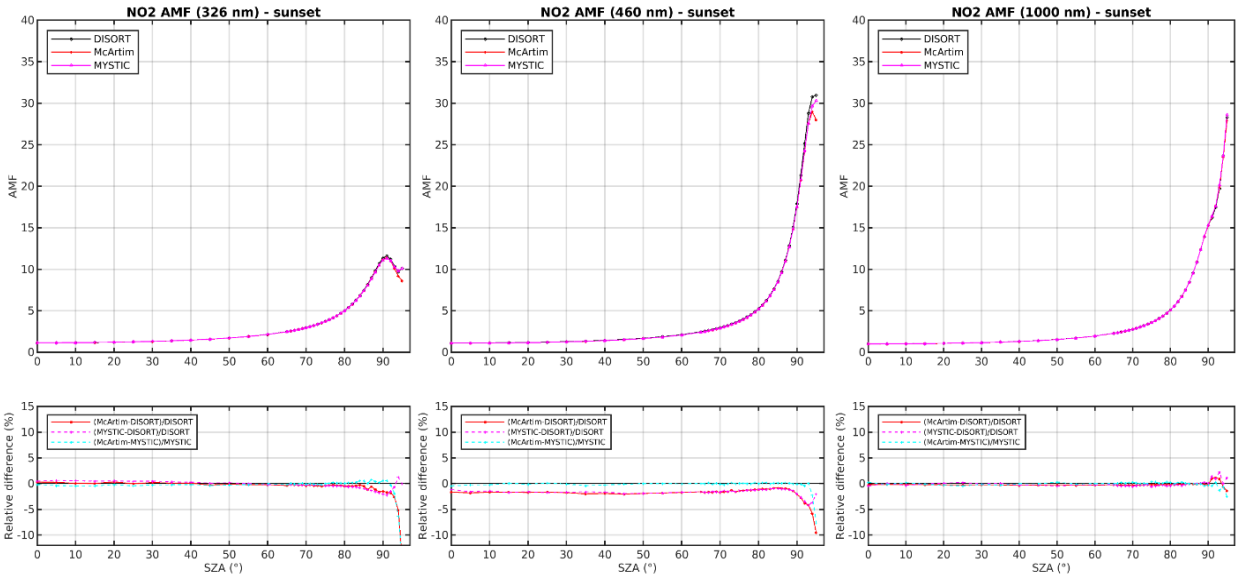

Figure 5: NO_2 AMF comparison results at 326 (left), 460 (middle), and 1000 nm.

As can be seen, a very good consistency is obtained between both full spherical codes (McArtim v3 and MYSTIC), with NO_2 AMF relative difference close to 0% except at very large SZAs. The comparison between McArtim/MYSTIC and DISORT NO_2 AMF at 460 nm shows an impact of the sphericity at 460nm of about 1.5% below 85°SZA and up to 2-3% between 90° and 93°SZA. A similar impact of the sphericity is also found when comparing LIDORT to McArtim/MYSTIC (not shown here). The impact of the sphericity decreases at UV wavelengths (326 nm) due to the larger contributions of Rayleigh scattering and ozone absorption, which both lead to shorter horizontal paths for diffuse light and thus a weaker effect of the sphericity. The comparison at 1000 nm is representative of single scattering conditions (i.e. only direct light) and from Figure 5, we see that spherical and pseudo-spherical models agree very well.

Overall, the good consistency between DISORT, MYSTIC, McArtim v3, but also LIDORT indicates that DISORT is appropriate to be used as forward model in the stratospheric NO_2 profiling. Since sensitivity tests have shown that including a correction for the sphericity can sometimes reduce the amplitude of the double peak pattern (see Figure 6), our recommendation is to implement this correction in the consolidated version of the profiling algorithm based on the difference as a function of the SZA between DISORT and McArtim v3 NO_2 AMFs (see middle plot in Figure 5; see also Deliverable D-1.5).

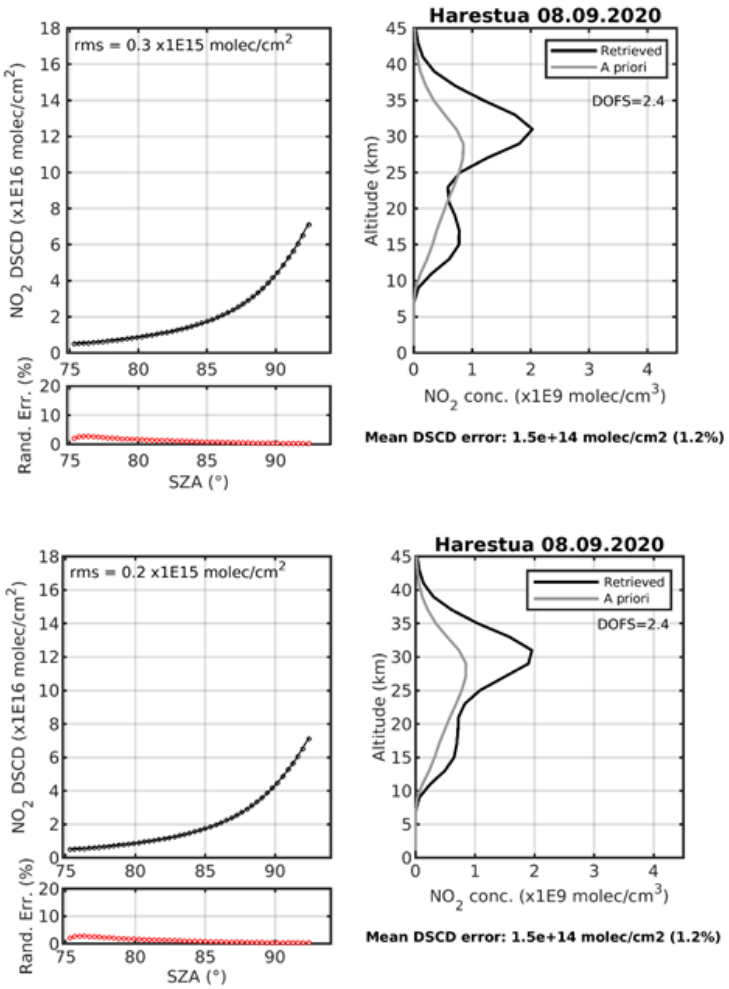

Figure 6: Examples of a retrieval (Harestua 08/09/2020 sunrise) without (upper plots) and with (lower plots) applying a correction for the sphericity. In this example, the RMS is slightly reduced when the sphericity correction is applied, while the DOFS value does not change.

3.2.2 Impact of the photochemical correction included in the forward model

3.2.2.1 Sensitivity tests on averaging a priori profiles and photochemical correction

In the current version of the stratospheric NO_2 profiling algorithm, the profiles are retrieved at 90°SZA sunrise and sunset. The weighting functions (WF) are therefore normalised as follows in order to be representative of the photochemical conditions at 90°SZA:

$$WF_{pc}(z,sza) = WF(z,sza)*[NO_2]_{z,sza}/[NO_2]_{z,90°}$$

where WF_{pc} is the photochemically-corrected WF, z is the altitude and $[NO_2]$ is the NO_2 concentration at a given altitude and SZA.

So far, daily WF and NO_2 profiles are extracted from look-up tables based on the day number of the year corresponding to the selected measurements. Based on previous work, it was found that a priori profiles sometime show discontinuities that can influence the retrieved profile shape. To investigate this issue, test retrievals were performed using a priori profiles and photochemical corrections

averaged over the day number of measurement +/- 15 days period. Figure 7 shows that this averaging can stabilize the retrieval and lead to smoother and likely more realistic profile shapes.

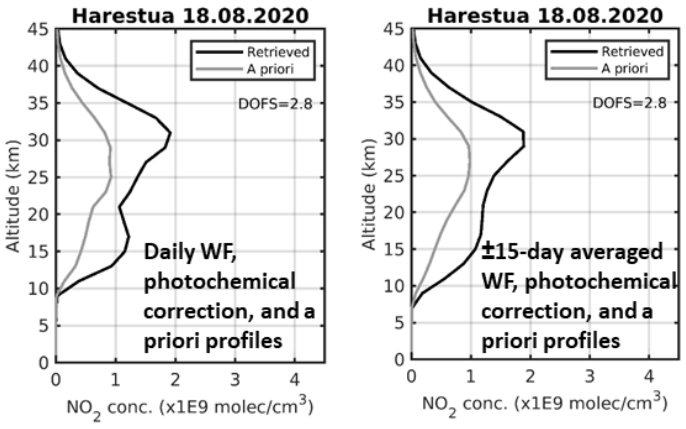

Figure 7: Examples of retrieval (Harestua 18/08/2020 sunrise) using daily (left plot) and ±15-day averaged (right plot) WF, photochemical correction and a priori profiles.

3.2.2.2 Sensitivity tests on uncertainties related to photochemical model simulations

The impact of the simulated twilight photochemical variations of the NO_2 profile on the double peak patterns that are sometimes obtained in the retrieved stratospheric NO_2 profiles at the remote Harestua station has been further investigated. Sensitivity tests have shown that the current twilight NO_2 photochemistry simulated by the PSCBOX model (standard run) seems to be not optimal in some conditions. In these tests, the twilight NO_2 variation with respect to 90° SZA (which is the retrieval SZA) has been artificially slowed down and speeded up (see Figure 8). As illustrated in Figure 9, it is found that a slower NO_2 variation with respect to 90°SZA tends to reduce the amplitude of the double peak pattern and to therefore stabilize the retrieval. In contrast, a faster photochemical variation leads to an increase of the double peak pattern amplitude.

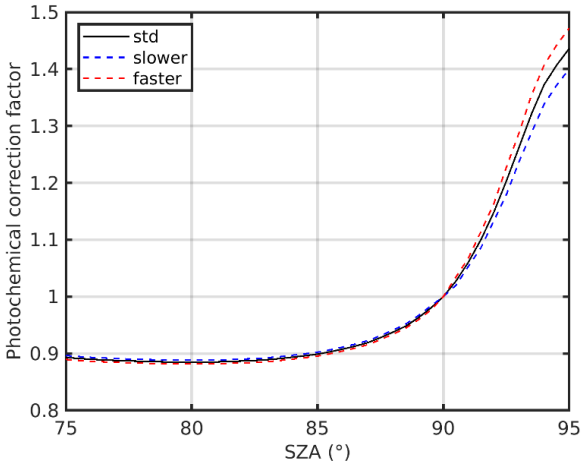

Figure 8: twilight NO_2 vertical column density variation normalised with respect to 90° SZA. Black solid line: standard photochemical box-model run, blue and red dashed lines: slower and faster photochemical variations with respect to the standard box-model run, respectively.

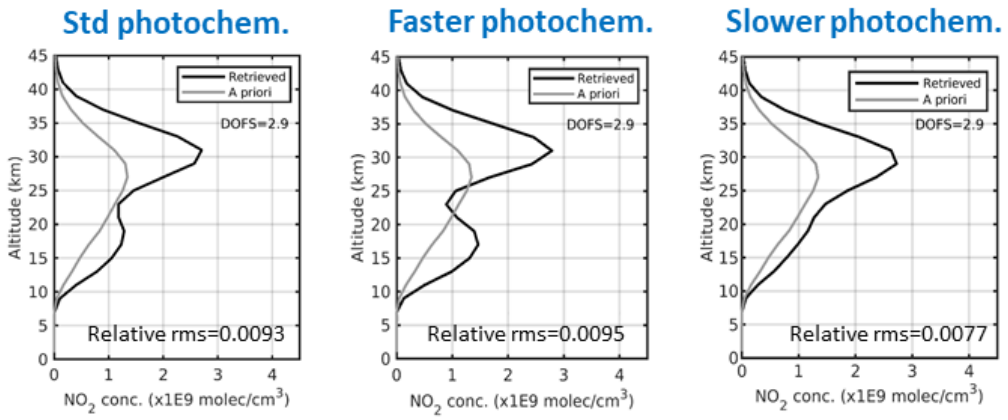

Figure 9: Impact of faster (middle) and slower (right) twilight NO_2 variations on the retrieved profile shape (Harestua 10.09.2020 sunset retrieval). Retrieval results corresponding to the standard photochemistry appear in the left plot.

Sensitivity tests on kinetic rate constant uncertainties of some key reactions involving NO_2 have been performed using the photochemical box-model PSCBOX in order to determine which chemical or photolysis reaction(s) and related uncertainty can mimic a slower twilight NO_2 variation compared to the standard model run. PSCBOX model was initialised with SLIMCAT chemical and meteorological fields corresponding to the Harestua station and uncertainties on the reaction rates were taken from the JPL Evaluation n°19-5 (Burkholder et al., 2020). The reactions included in this exercise are:

<u>Photolysis reactions:</u>

$NO_2 + h\nu \Rightarrow NO + O$

$NO_3 + h\nu \Rightarrow NO_2 + O$

$NO_3 + h\nu \Rightarrow NO + O2$

$N_2O_5 + h\nu \Rightarrow NO_2 + NO_3$

$HNO_3 + h\nu \Rightarrow OH + NO_2$

$HNO_4 + h\nu \Rightarrow HO_2 + NO_2$

$HNO_4 + h\nu \Rightarrow OH + NO_3$

$ClONO_2 + h\nu \Rightarrow ClO + NO_2$

$ClONO_2 + h\nu \Rightarrow Cl + NO_3$

$BrONO_2 + h\nu \Rightarrow BrO + NO_2$

<u>Bimolecular reactions:</u>

$NO + O_3 \Rightarrow NO_2 + O_2$

$NO_2 + O_3 \Rightarrow NO_3 + O_2$

<u>Termolecular reactions:</u>

$NO_3 + NO_2 + M \Rightarrow N_2O_5$

$ClO + NO_2 + M \Rightarrow ClONO_2$

$BrO + NO_2 + M \Rightarrow BrONO_2$

<u>Equilibrium reactions:</u>

$N_2O_5 <=> NO_2 + NO_3$

Among all these reactions, only the NO_2 photolysis rate has been found to have a significant impact on the twilight NO_2 concentration variation. Figure 10 shows that reducing this photolysis rate by 10% (which is consistent with the uncertainties on NO_2 cross sections and photodissociation quantum yield according to the JPL Evaluation n°19-5) leads to a slower twilight NO_2 VCD variation similar to the one mimicked in Figure 8.

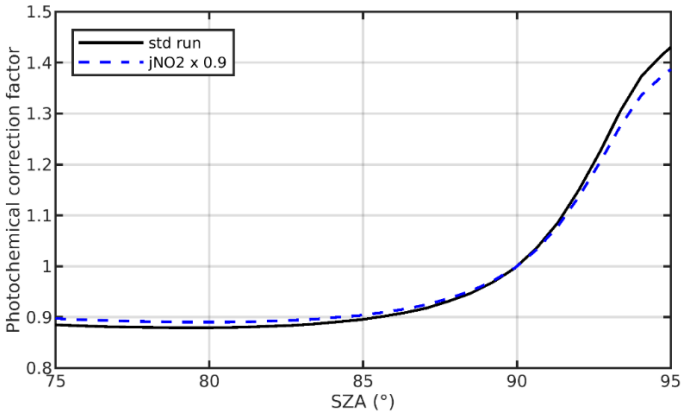

Figure 10: Impact of reducing the photolysis rate of NO_2 by 10% on the sunrise NO_2 vertical column density diurnal variation normalised with respect to 90°SZA. The black dashed line corresponds to the twilight NO_2 vertical column density diurnal variation extracted from the standard photochemical box model run.

For the consolidated algorithm, new photochemical box model simulations will be performed using jNO_2 x 0.9. The corresponding new NO_2 profile diurnal variations will then be used to calculate updated weighting functions.

3.3 Approach 3: Characterization of the 'atmospheric noise' related to clouds and tropospheric NO_2

3.3.1 Use of the extra-DSCD error approach

An extra-DSCD error approach has been developed for improving the stability of the stratospheric NO_2 profile retrieval in the case of low to moderate tropospheric NO_2 contamination. As shown in Figure 11, the approach is based on the differences between measured and calculated NO_2 DSCDs and includes the following steps:

1. A first profile retrieval is performed using the standard DOAS fit error for the construction of the measurement noise matrix S_ε.
2. At each SZA, calculation of the extra-DSCD error (EDE_{SZA}), which is the absolute difference between measured DSCD and the one recalculated using the retrieved profile: $EDE_{SZA} = abs(DSCD_{SZA,\,meas} - DSCD_{SZA,\,calc})$
3. For SZA(s) at which the EDE_{SZA} is larger than the DOAS fit error by a given threshold (factor of 10 in the present case), EDE_{SZA} is used instead of the DOAS fit error for the construction of a new S_ε.This new S_ε is then used in a second profile retrieval step.

This EDE approach has been tested on measurements from the Bremen station. This site if often affected by moderate pollution events. As illustrated in Figure 12, the EDE approach generally stabilizes the

retrieved profiles in the case of low to moderate tropospheric NO_2 contamination (less marked or disappearance of double peaks or other unrealistic patterns).

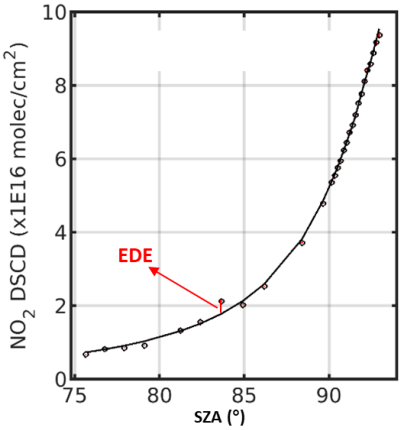

Figure 11: Illustration of the EDE approach developed for the stratospheric NO_2 profile retrieval.

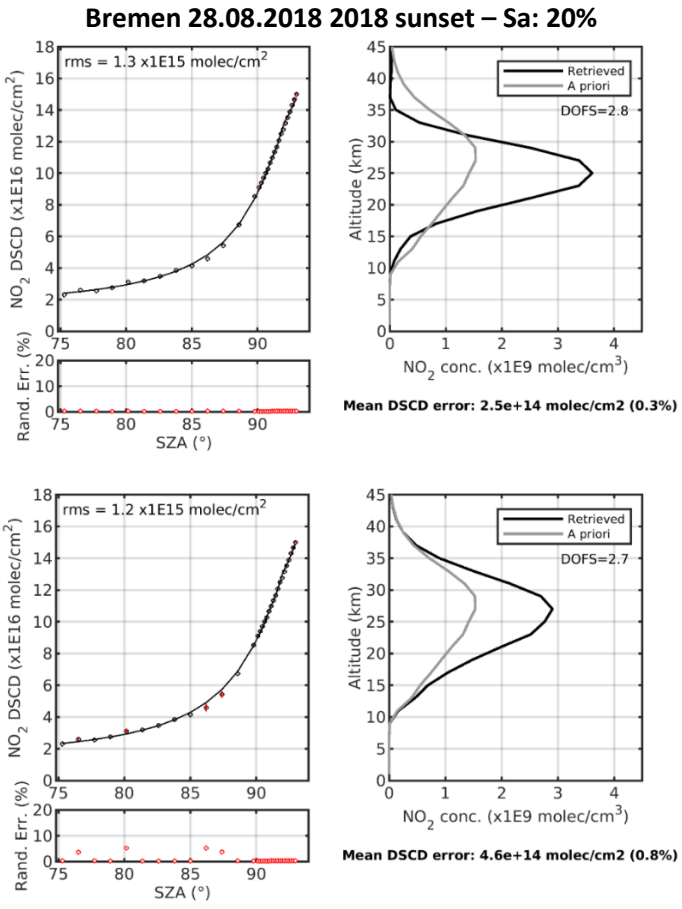

Figure 12: Example of stabilization of the retrieved profile shape when applying the EDE approach (measurements from Bremen high SNR instrument on 28/08/2018 sunset). The top and bottom panels correspond to retrieval results without and with application of the EDE approach, respectively. The random errors in red are those used for the construction of the S_ε matrix.

As verification purpose, the derived extra-DSCD errors have been also compared to the NO_2 natural variability estimated from fast-zenith measurements. This has been done at the Bremen site where fast-zenith measurements (Avantes CCD with quartz fiber; 10s total integration time) were performed in parallel to the main instrument during the 1-8 March 2022 period. An example of the comparison between both types of measurements is shown in Figure 13. As can be seen, the NO_2 DSCD fit errors largely underestimate the NO_2 variability in the 75-85°SZA interval (interval where the effect of a tropospheric contamination is expected to be the largest). In contrast, when the EDE is added in quadrature to the NO_2 DSCD fit errors, a good consistency is found on average with the NO_2 natural variability estimated from fast-zenith measurements. This indicates that the EDE approach provides a reasonable estimate of the atmospheric noise related to low to moderate tropospheric NO_2 pollution events.

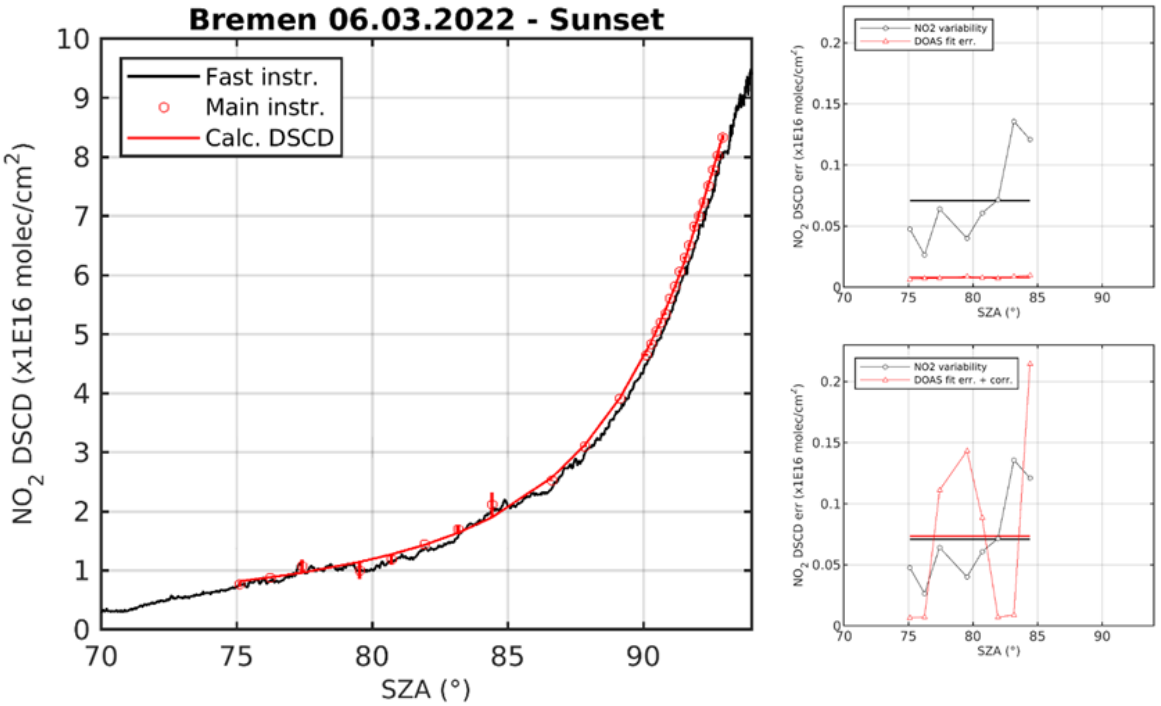

Figure 13: (left plot) - Comparison between fast-zenith NO_2 DSCD measurements (435-490 nm fitting window) and NO_2 DSCDs measured with the main instrument (425-490 nm fitting window). (Right plots) – Comparison of the NO_2 DSCD errors from the main instrument (upper plot: retrieval with only DOAS fit errors; lower plot: retrieval with DOAS fit errors and EDE) with the NO_2 natural variability from the fast-zenith measurements. This NO_2 natural variability is derived at each main instrument NO_2 DSCD measurement time by taking the standard deviation of all fast measurements comprised in the $[t_{main,\,n} - (t_{main,\,n} - t_{main,\,n-1})/2 \;\; t_{main,\,n} + (t_{main,\,n+1} - t_{main,\,n})/2]$ time interval.

This verification exercise also shows that, in low to moderate pollution conditions, having a fast-zenith spectrometer operating in parallel to the main standard instrument could be an added value for better characterizing the atmospheric noise related to the tropospheric NO_2 contaminations and therefore for improving the stratospheric NO2 profile retrieval in terms of QA/QC.

4 Overall assessment and recommendations

The sensitivity tests performed so far for investigating the presence of double peak patterns in the retrieved stratospheric NO_2 profiles and for better estimating the uncertainty on the NO_2 DSCDs have been based on study cases involving a limited number of measurement days at the Harestua and Bremen stations.

In order to fully assess the suggested approaches for consolidating the quality of the profile retrievals, the following sensitivity tests have been extended on a longer time period (May-September where stratospheric NO_2 shows the largest abundance):

- Taking ±15-day averaged WF, photochemical correction, and a priori profiles instead of daily data
- Implementation of slower twilight NO2 photochemical variation
- Implementation of the EDE approach

The statistics on successful retrievals are presented in Figure 14. Successful retrievals are those passing the current QA/QC checks implemented in the CPS, i.e. DOFS and RMS of the difference between measured and recalculated NO_2 DSCDs smaller than pre-defined thresholds and retrieved profiles must not display negative values. The fourth QA/QC test (rejection of the profiles with a double peak pattern) is de-activated in order to make statistics on the number of profiles with double peaks and quantify the impact of the three above consolidation steps on this number.

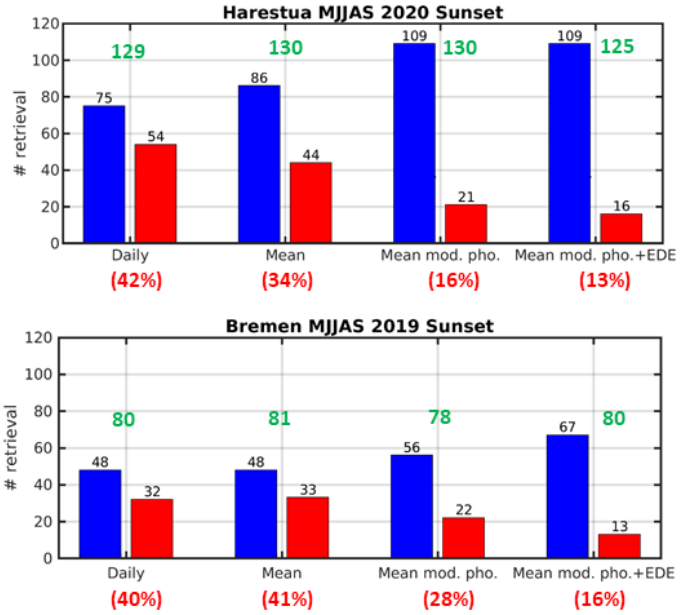

Figure 14: Statistics on the presence of double peak pattern in the retrieved profiles after implementation of the different consolidation steps. 'Daily' scenario corresponds to standard retrieval with the current version of the algorithm (baseline scenario). 'Mean' scenario corresponds to the implementation of the mean WF, photochemical correction, and a priori profiles. 'Mean mod. pho.' corresponds to the 'Mean' scenario + implementation of slower twilight photochemistry. 'Mean mod. pho. + EDE' corresponds to the 'Mean mod. pho.' scenario + implementation of the EDE. Red and blue bars denote the number of retrieved profiles with and without a double peak pattern, respectively. The numbers in green are the numbers of retrievals that successfully passed the first three QA/QC checks). The percentage values between brackets correspond to the percentages of profiles with double peak with respect to the total number of profiles successfully passing the first three QA/QC checks.

At the Harestua station, it is found that the use of a slower NO_2 photolysis rate in the box-model simulations tends to significantly reduce the number of retrieved profiles with a double peak pattern. A similar feature is obtained at the Bremen site, although at this station, the application of the extra-DSCD error correction seems to play a more significantly role in the reduction of profiles with double peak than a slower NO_2 photochemical variation. This is due to the fact that Bremen measurements are much more affected by tropospheric NO_2 contaminations than Harestua which is located in a remote area. The use of averaged WF, photochemical correction, and a priori leads also to a decrease of the number of profiles with double peak at the Harestua site but not at Bremen.

The impact on these three consolidation steps on the retrieved VCDs has been also investigated (not shown here; see presentation on WP1 status by F. Hendrick at the PM3 meeting) and it is found that this impact is small (<2%).

Based on this statistical analysis, our recommendation for the upgrade version of the profiling algorithm is to implement all the three consolidation approaches + the correction for the sphericity (see Sect. 3.2.1). The way they should be implemented in the CPS is described in the Deliverable D-1.5 (TIP). The application of these recommendations to other profile retrievals (e.g. BrO) should be also investigated in the future. However, it is beyond the scope of the present project.

5 References

Bogumil, J., et al., Temperature dependent absorption cross sections of O_3, NO_2, and other atmospheric trace gases measured with the SCIAMACHY spectrometer, Proc. ERS - Envisat Symposium. Looking down at our Earth in the New Millennium, Gothenburg 16 - 20 October 2000.

Burkholder, J. B., et al., Chemical Kinetics and Photochemical Data for Use in Atmospheric Studies, Evaluation n°19, NASA JPL Publication n° 19-5, 2020.

Burrows, J. P., et al., Atmospheric Remote-Sensing Reference Data from GOME: 1. Temperature-Dependent Absorption Cross Sections of NO_2 in the 231-794 nm Range, J. Quant. Spectrosc. Radiat. Transfer**,** 60, 1025-1031, 1998.

Emde, C., Yu, H., Kylling, A., van Roozendael, M., Stebel, K., Veihelmann, B., and Mayer, B.: Impact of 3D cloud structures on the atmospheric trace gas products from UV–Vis sounders – Part 1: Synthetic dataset for validation of trace gas retrieval algorithms, Atmos. Meas. Tech., 15, 1587–1608, https://doi.org/10.5194/amt-15-1587-2022, 2022.

Hendrick, F., Barret, B., Van Roozendael, M., Boesch, H., Butz, A., De Mazière, M., Goutail, F., Hermans, C., Lambert, J.-C., Pfeilsticker, K., and Pommereau, J.-P.: Retrieval of nitrogen dioxide stratospheric profiles from ground-based zenith-sky UV-visible observations: validation of the technique through correlative comparisons, Atmos. Chem. Phys., 4, 2091–2106, 2004, http://www.atmos-chem-phys.net/4/2091/2004/.

Mayer, B., and A. Kylling, Technical note: The libRadtran software package for radiative transfer calculations - description and examples of use, Atmos. Chem. Phys., 5, 1855-1877, 2005.

Spurr, R., VLIDORT: A linearized pseudo-spherical vector discrete ordinate radiative transfer code for forward model and retrieval studies in multilayer multiple scattering media, Journal of Quantitative Spectroscopy & Radiative Transfer, pp. 316-342, 2006.

Vandaele, A. C., et al., Measurements of the NO_2 absorption cross section from 42000 cm-1 to 10000 cm-1 (238-1000 nm) at 220 K and 294 K, J. Quant. Spectrosc. Radiat. Transfer, 59, 171-184, 1998.